

# JGR Space Physics

## RESEARCH ARTICLE

10.1029/2021JA029544

### Key Points:

- Magnetic reconnection can happen a few planetary radii from Jupiter when its magnetic field is locally sheared on plasma kinetic scales
- While negligible at weakly magnetized planets, reconnection electric fields near Jupiter's poles can be as strong as in the solar corona
- These reconnection events could generate high-energy electron beams, contributing to an explanation for Jupiter's mysterious polar auroras

### Supporting Information:

Supporting Information may be found in the online version of this article.

### Correspondence to:

A. Masters,  
[a.masters@imperial.ac.uk](mailto:a.masters@imperial.ac.uk)

### Citation:

Masters, A., Dunn, W. R., Stallard, T. S., Manners, H., & Stawarz, J. (2021). Magnetic reconnection near the planet as a possible driver of Jupiter's mysterious polar auroras. *Journal of Geophysical Research: Space Physics*, 126, e2021JA029544. <https://doi.org/10.1029/2021JA029544>

Received 8 MAY 2021  
Accepted 28 JUN 2021

## Magnetic Reconnection Near the Planet as a Possible Driver of Jupiter's Mysterious Polar Auroras

A. Masters<sup>1</sup> , W. R. Dunn<sup>2,3</sup> , T. S. Stallard<sup>4</sup> , H. Manners<sup>1</sup> , and J. Stawarz<sup>1</sup> 

<sup>1</sup>Blackett Laboratory, Imperial College London, London, UK, <sup>2</sup>Department of Space and Climate Physics, Mullard Space Science Laboratory, University College London, Surrey, UK, <sup>3</sup>The Centre for Planetary Sciences at UCL/Birkbeck, London, UK, <sup>4</sup>Department of Physics and Astronomy, University of Leicester, Leicester, UK

**Abstract** Auroral emissions have been extensively observed at the Earth, Jupiter, and Saturn. These planets all have appreciable atmospheres and strong magnetic fields, and their auroras predominantly originate from a region encircling each magnetic pole. However, Jupiter's auroras poleward of these "main" emissions are brighter and more dynamic, and the drivers responsible for much of these mysterious polar auroras have eluded identification to date. We propose that part of the solution may stem from Jupiter's stronger magnetic field. We model large-scale Alfvénic perturbations propagating through the polar magnetosphere toward Jupiter, showing that the resulting  $<0.1^\circ$  deflections of the magnetic field closest to the planet could trigger magnetic reconnection as near as  $\sim 0.2$  Jupiter radii above the cloud tops. At Earth and Saturn this physics should be negligible, but reconnection electric field strengths above Jupiter's poles can approach  $\sim 1 \text{ V m}^{-1}$ , typical of the solar corona. We suggest this near-planet reconnection could generate beams of high-energy electrons capable of explaining some of Jupiter's polar auroras.

**Plain Language Summary** When energetic particles from space hit a planet's upper atmosphere the resulting chemistry can produce light, leading to spectacular "auroras." Jupiter is the largest planet in the Solar System, with the strongest magnetic field generated in its interior, and with the brightest auroras. We understand why Jupiter's auroras are so bright to a large extent, but a long-standing mystery is what causes the swirling auroras around Jupiter's poles, which we do not see at other planets. We present a new idea that might lead to a solution to this problem. We show that under certain conditions in space just above Jupiter's polar atmosphere some of the energy stored in the planet's magnetic field can be released, possibly accelerating particles and producing auroras below. If this idea is supported by future research it would imply that Jupiter's bright polar auroras are due to the planet's very strong magnetic field, with implications for similarly strongly magnetized planets in orbit around distant stars.

## 1. Introduction

Auroral emissions have been extensively observed at three planets in our solar system: the Earth, Jupiter, and Saturn. All these planets have both appreciable atmospheres and internally generated magnetic fields. Auroral photons primarily originate from a region encircling each magnetic pole at all three of these planets and are generally due to the chemistry resulting from charged particles precipitating into the atmosphere from space. Jupiter stands out as not only having the brightest emissions, but also as having brighter and highly dynamic auroras poleward of its "main" emissions, as shown in Figure 1a (Badman et al., 2015; Bhardwaj & Gladstone, 2000; Grodent, 2015; Miller et al., 2000; Prangé, 1992; Waite et al., 2000). While much progress has been made in explaining the main Jovian emission as the result of particles accelerated by quasi-static magnetic-field-aligned electric fields and/or wave-particle interactions in the surrounding magnetosphere space environment (e.g., Cowley & Bunce, 2001; Hill, 2001; Mauk et al., 2017; Saur et al., 2018), explanations for the polar auroras have been more elusive.

Jupiter's polar auroras are brightest in the ultraviolet (UV), providing near-instantaneous measurements of the fluxes of precipitating electrons that are responsible (Bonfond et al., 2017; Gérard et al., 2019; Grodent et al., 2003, 2018; Nichols, Clarke, Gérard, & Grodent, 2009; Nichols, Clarke, Gérard, Grodent, & Hansen, 2009; Stallard et al., 2016). The polar regions are often divided up into a "dark" region at dawn

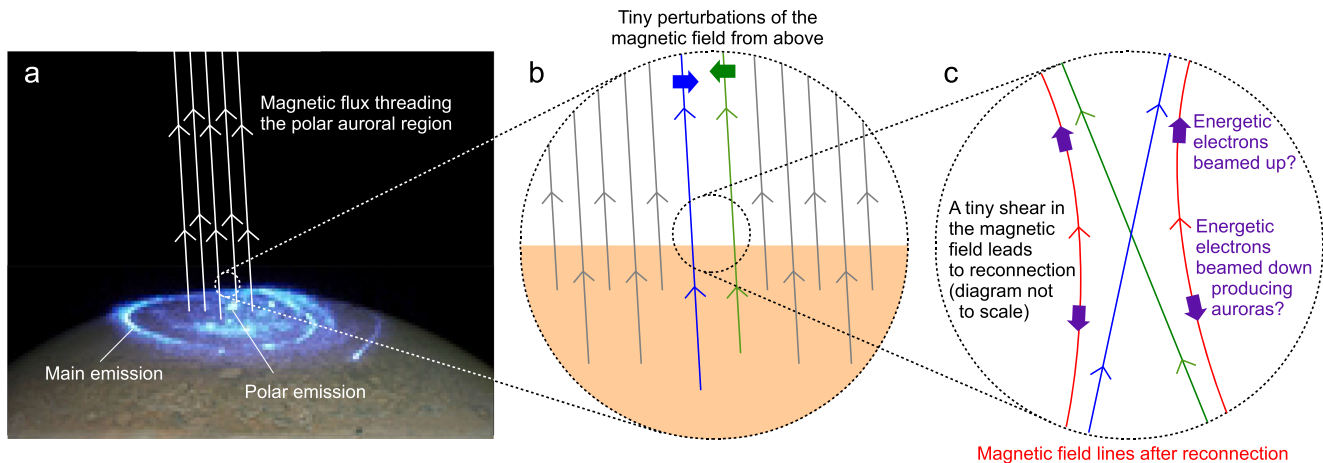


**Figure 1.** Jupiter’s ultraviolet (UV) auroras and a summary of our possible explanation for some of the polar emissions. (a) A snapshot of the UV auroras superposed on top of a visible image of Jupiter, credit NASA, ESA, and J. Nichols (University of Leicester), with annotation added in white. Our proposed explanation is illustrated in (b) and (c). In all panels the arrowed lines are paths through Jupiter’s vector magnetic field (magnetic field lines).

that is generally devoid of emission, “active” regions just poleward of the main emission at noon and dusk, and a “swirl” region at the highest magnetic latitudes (e.g., Grodent et al., 2003). Polar auroral morphology is diverse and transient, evolving on timescales as short as minutes or even seconds. These include relatively powerful and short-lived emissions from active regions, periodic spots and expanding circles of emission near the boundaries of the swirl regions, and “turbulent” evolving features that are often swirl-like within the aptly named swirl regions themselves (e.g., Grodent et al., 2003; Haewsantati et al., 2021; Hue et al., 2021).

The precipitating electrons in Jupiter’s polar regions are typically more energetic than those associated with other auroral features (Gérard et al., 2019; Paranicas et al., 2018). Recent particle observations made a few planetary radii above the polar atmosphere by the *Juno* spacecraft provide important clues about the drivers of the polar emissions. Beams of electrons traveling away from the planet (upward) along Jupiter’s magnetic field have been persistently detected poleward of the main emissions, with observed electron energies of order  $\sim 10$  keV to  $\sim 1$  MeV (Clark et al., 2017; Ebert et al., 2017, 2019; Mauk et al., 2020) and also evidence for electrons in the MeV range (Bonfond et al., 2018; Paranicas et al., 2018). These beams have been attributed to either a broadband acceleration mechanism or quasi-static planetward (downward) magnetic-field-aligned electric fields below the spacecraft, with an important role played by subsequent whistler wave-particle interactions (Elliott, Gurnett, Kurth, Clark, et al., 2018; Elliott, Gurnett, Kurth, Mauk, et al., 2018; Elliott, Gurnett, Yoon, et al., 2020).

In isolation, downward magnetic-field-aligned electric fields below the spacecraft appear to be consistent with the expected downward magnetic-field-aligned electric currents across the polar regions (Cowley et al., 2003). However, downward ion fluxes suggest that such quasi-static electric fields are also generally present above the spacecraft (Mauk et al., 2020), similarly consistent with the expected currents. The primary reasons for upward electron acceleration close to the planet are therefore unclear, and none of this directly reveals how polar auroras are generated below.

Discrete auroral features in the active regions and the edges of the swirl regions could magnetically map to the boundary of the magnetosphere and may be explainable as the result of more localized examples of the same physics that is thought to produce the main emissions (e.g., Hue et al., 2021), but these established drivers do not appear to be able to make sense of the particle observations made above the broader swirl regions. The lack of persistently observed downward electron beams or wider particle evidence for upward magnetic-field-aligned currents suggests that an unidentified downward-electron-acceleration mechanism is operating closer to the planet.

Here we suggest that this mechanism could be magnetic reconnection occurring in the near-planet polar magnetosphere, implying that Jupiter’s brighter polar auroras compared to Earth and Saturn may be a

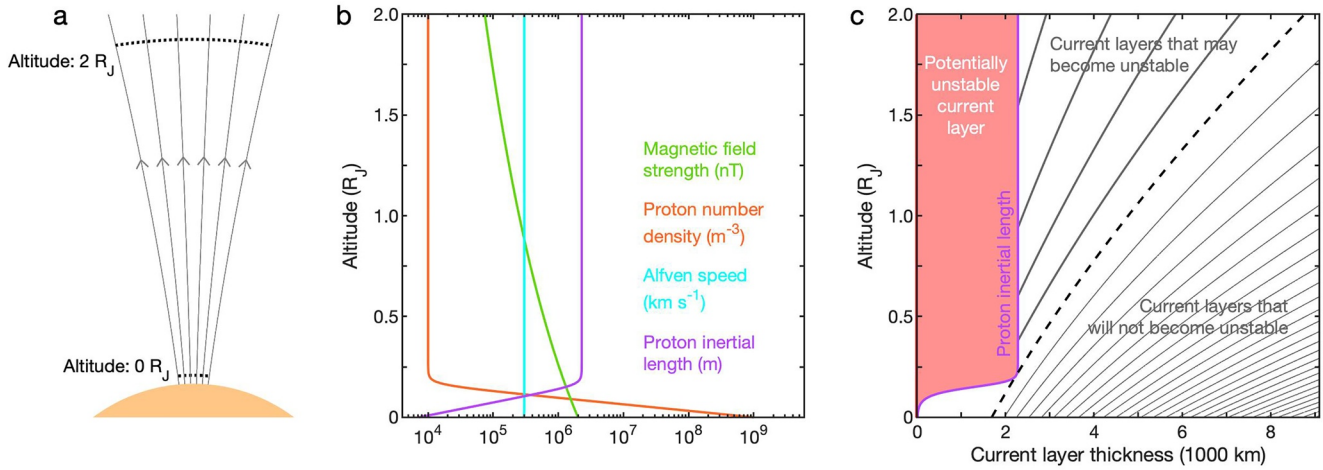


**Figure 2.** The model domain and its magnetized plasma properties. (a) Modeled altitude range above the northern swirl region. Jupiter’s dipole magnetic field lines are shown in gray. (b) Profiles of magnetized plasma parameters with altitude along any chosen field line. (c) Curves representing the altitude-dependent thickness of example current layers introduced at an altitude of 2  $R_J$ . Thicker gray curves correspond to current layers whose thickness falls below the proton inertial length somewhere below an altitude of 2  $R_J$ , thinner gray curves represent current layers whose thickness is above the proton inertial length throughout, and the dashed curve indicates the boundary between these two regimes in this parameter space.

consequence of Jupiter’s considerably stronger magnetic field. The aim of this paper is to outline the idea and make an argument for plausibility based on energetics.

## 2. Modeling

The basis of our theory comes from simple modeling of the magnetized charged particle (plasma) environment above the swirl regions of Jupiter’s atmosphere, which we refer to as the near-planet polar magnetosphere. We consider paths through the planet’s polar magnetic field (“magnetic field lines”), and use a one-dimensional (1-D), relativistic, ideal magnetohydrodynamic (MHD) model when assessing how the shape of a single field line evolves with time. In the latter modeling, the single spatial dimension is aligned with an individual field line.

We model a spatially limited section of field lines above the northern swirl region, as shown in Figure 2a. The broad conclusions we draw also apply to the southern hemisphere. We set the lower limit of our domain at a zero-level of altitude, defined as the boundary above which inter-particle collisions are effectively absent. We choose an upper limit at an altitude of 2 Jupiter radii ( $R_J$ , 1  $R_J = 71,492$  km) to approximate the lowest altitude at which spacecraft observations have been made (e.g., Mauk et al., 2020). Below an altitude of 0  $R_J$  is the bulk of the atmosphere, and above an altitude of 2  $R_J$  is the more distant magnetosphere. Note that the unit of  $R_J$  that we use applies to the planet’s equatorial radius, which is larger than the polar radius. Nonetheless, we use this value to be consistent with recent magnetospheric studies, and because it provides a unit of reference that is sufficiently accurate for our purposes.

Descriptions of how key parameters are assumed to vary with altitude along the modeled part of all polar magnetic field lines are shown in Figure 2b. We take Jupiter’s magnetic field strength at an altitude of 0  $R_J$  to be  $2 \times 10^6$  nT and assume an inverse cubic dependence on distance from the center of the planet that is consistent with the magnetic dipole (Connerney et al., 2018). We assume the plasma is charge-neutral and comprised of electrons and protons (heavier ions are strongly confined to the equatorial regions [e.g., Bagenal, 1992]). Our profile of proton number density ( $n_p$ ) is based on radio occultations of Jupiter’s atmosphere (e.g., Hinson et al., 1997). We set the peak value at an altitude of 0  $R_J$  to be  $10^9\ m^{-3}$  and assume an exponential decrease over a scale height ( $H$ ) of 1,000 km, tending to a limiting density of  $10^4\ m^{-3}$  in the magnetosphere above (Saur et al., 2018). This can be expressed as a function of altitude ( $z$ ) as

$$n_p = \left(10^9\right) e^{-\frac{z}{H}} + \left(10^4\right)$$

This density and the strength of Jupiter’s magnetic field ( $B$ ) allow us to determine the speed of the Alfvén waves ( $v_A$ ) that propagate along the magnetic field as transverse perturbations of the magnetic field and bulk plasma velocity. In Jupiter’s polar magnetosphere this speed is relativistic, expressed as

$$v_A = \frac{\left( \frac{B}{\sqrt{\mu_0 \rho}} \right)}{\sqrt{1 + \left( \frac{B}{c \sqrt{\mu_0 \rho}} \right)^2}}$$

where  $\mu_0$  is the permeability of free space,  $\rho$  is the plasma mass density, and  $c$  is the speed of light. The high field strength compared to plasma mass density makes the Alfvén speed approximately the speed of light at all modeled altitudes. Lastly, the proton number density sets the proton plasma frequency at which protons will oscillate in response to a local electric charge imbalance, which defines the proton inertial length. This is the largest of the plasma “kinetic” scales that characterize the environment, varying from order 10 km at an altitude of 0  $R_J$  to order 1,000 km at an altitude of  $\sim 0.25 R_J$ , and then remaining approximately constant in the magnetosphere above.

We define our theory that potentially explains some of the polar auroras by considering what will happen if we perturb the modeled length of polar magnetic field lines from above. Beyond an altitude of 2  $R_J$  the magnetic field maps to the outermost regions of Jupiter’s magnetosphere, likely interacting with the flow of solar wind plasma from the Sun and forming the planet’s magnetic tail that extends anti-sunward to approximately the orbit of Saturn (e.g., Behannon et al., 1983; Cowley et al., 2003; Delamere & Bagenal, 2010; Isbell et al., 1984; Zhang et al., 2021). This is a highly dynamic magnetized plasma environment with typical flow speeds of order 100 km s<sup>-1</sup>, launching Alfvénic disturbances that propagate toward the model domain from above. We can treat the larger-scale effects by introducing constant-altitude perturbations of the coupled plasma and magnetic field at points on polar field lines that lie at the upper boundary of the domain, at an altitude of 2  $R_J$ . We hereafter refer to these as “upper-boundary points.”

The upper-boundary points of polar field lines define an upper-boundary surface, across which conditions will be dynamic and inhomogeneous. Figure 2c explores what will happen when adjacent bundles of magnetic field lines at this boundary are subject to different time-dependent displacements. By Ampère’s law, a layer of electric current will be present between the two field regimes, and as the Alfvénic disturbances propagate through the system to lower altitudes they will support the downward extension of these current layers. In Figure 2c a number of example current layers are considered, introduced with different thicknesses at an altitude of 2  $R_J$ . We approximate the variation of layer thickness with altitude by considering a circular contour at a constant altitude, moving it in altitude while varying its radius to ensure the same amount of magnetic flux threads through it. Because dipole field strength with distance from the center of the planet ( $R$ ) scales as  $B \propto R^{-3}$ , the radius of the circular contour ( $r$ ) will scale as  $r \propto R^{3/2}$ . We assume that the thickness of current layers will be subject to the same scaling as this contour.

It is apparent in Figure 2c that as current layers extend to lower altitudes by this assumed scaling they become progressively thinner as the magnetic field becomes stronger, as expected. Included in the panel is the proton inertial length. At thicknesses approximately at and below this scale a current layer may become unstable, leading to magnetic reconnection (e.g., Hesse & Cassak, 2020). This possibility underpins our theory concerning the origins of some of Jupiter’s polar auroras. Note that not all current layers extending through the system will become thin enough to reconnect, as illustrated by the range of examples shown in Figure 2c.

Magnetic reconnection involves the transfer of magnetic energy to charged particles. To quantify this, we can calculate the deflection of a magnetic field line that results from fixed-altitude displacement of its upper-boundary point. Consider the blue field line shown in Figure 1b, assume this field line points in the direction of increasing altitude, and define a transverse direction in which the upper-boundary point is displaced (the left-to-right direction in Figure 1b). The initially unperturbed (vertical) field line is shown in Figure 3a, extending through the model domain. If we now introduce uniform motion of the upper-boundary point on the field line at a speed of 50 km s<sup>-1</sup> then the evolving shape of the field line can be approximated by a solution to the classic 1-D wave equation that results from linearization of the equations of ideal

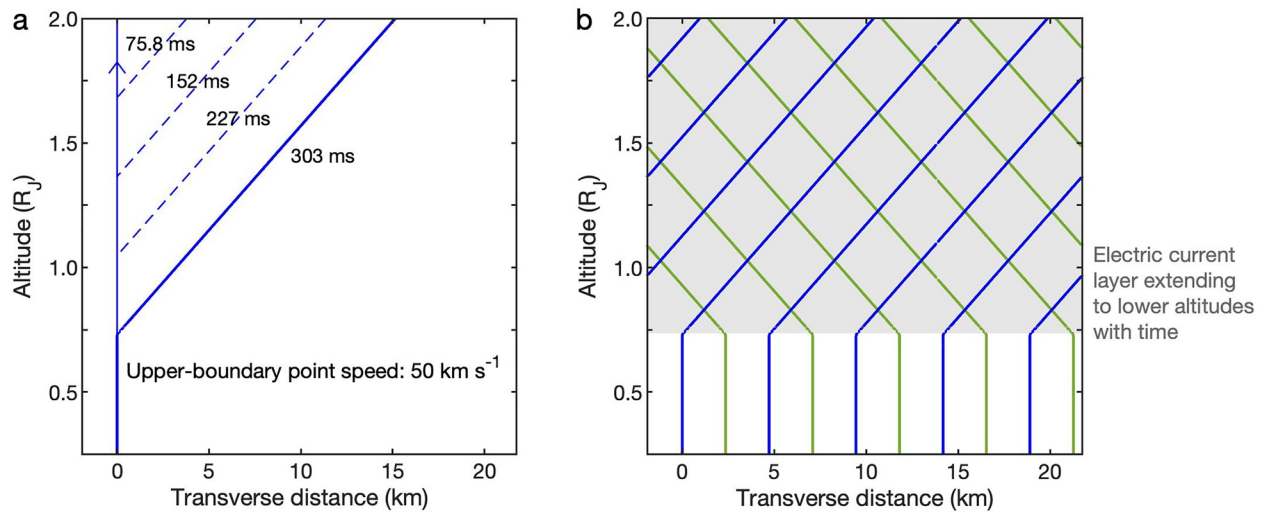


**Figure 3.** Modeling the deflection of magnetic field lines resulting from transverse displacement of their point at the upper-boundary altitude of  $2 R_J$ . (a) The evolving shape of a magnetic field line subject to left-to-right upper-boundary point motion at a speed of  $50 \text{ km s}^{-1}$ . The vertical field line corresponds to the start of the upper-boundary point motion and time elapsed is indicated for subsequent field line shapes. (b) A current layer resulting from opposing upper-boundary point motions. upper-boundary points of the blue field lines in the foreground are moving from left to right and upper-boundary points of the green field lines in the background are moving from right to left. All field lines correspond to 303 ms after the start of upper-boundary point motion.

MHD. Numerical solutions are shown in Figure 3a at different times elapsed since the introduction of the perturbation. These results are negligibly different from simply taking the field line deflection via the ratio of upper-boundary point displacement speed to the near-constant Alfvén speed.

The signal propagates to lower altitudes with time at relativistic speeds, deflecting the affected part of the field line at higher altitudes by  $0.01^\circ$  at all points. We obtain a mirror of these results if we consider the green field line shown in Figure 1b and subject it to the same perturbation, but in the opposite direction. Extension of this picture to consider a bundle of blue field lines in the foreground and a bundle of green field lines in the background is shown in Figure 3b. A layer of electric current lies within the page, between foreground and background, extending to lower altitudes with time. The thickness of this current layer is the distance between the foreground and background field lines in the out-of-page direction.

The results presented so far provide a relationship between the thickness of the current layer introduced from the more distant magnetosphere at the upper boundary (i.e., the spatial scale over which upper-boundary point motions are sheared) and the altitude at which reconnection may occur (see Figure 2c), and also allow us to quantify the magnetic field deflections (see Figure 3). Combining these results leads to the results presented in Figure 4, which shows a parameter space spanning the range of current layer thicknesses at the upper boundary that could lead to reconnection below, and up to  $100 \text{ km s}^{-1}$  shears between the motion of upper-boundary points on field lines. At each point in this parameter space reconnection could occur at a certain altitude, with a certain field deflection present. Figure 4a shows the magnitude of the transverse magnetic field component at this possible “reconnection altitude,” which is the reconnection magnetic field. Greater shears between upper-boundary point motions promote a stronger reconnection magnetic field, as do thicker current layers at an altitude of  $2 R_J$ . The latter is because thicker current layers lead to reconnection at the lowest altitudes where the magnetic field is strongest (see Figure 2c), with the caveat that current layer thicknesses above the upper limit of the range shown are not expected to lead to reconnection below.

Figure 4b shows the associated reconnection electric field strengths, also known as reconnection rates. These are products of the reconnection magnetic field strength, an Alfvén speed based on the reconnection magnetic field and local plasma mass density, and a 10% “reconnection efficiency” (e.g., Cassak & Shay, 2007). Conditions that promote higher reconnection electric field strengths are the same as those that promote higher reconnection magnetic field strengths. The topology of these possible reconnection events is illustrated in Figure 1c, where the antiparallel (reconnecting) magnetic field components are the

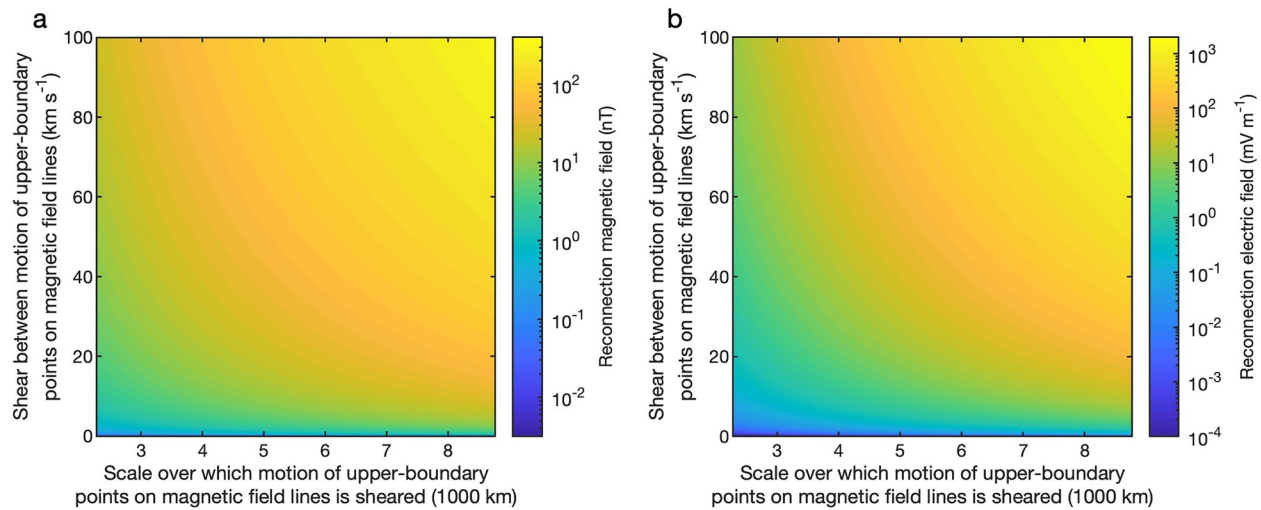


**Figure 4.** Predicted reconnection magnetic and electric field strengths at the altitudes where reconnection may occur. In all panels the x-axis refers to the motion of points on magnetic field lines at an altitude of  $2 R_J$  (upper-boundary points), and spans a range defined by the current layer thicknesses that could lead to reconnection (see Figure 2c). (a) Reconnection magnetic field strength. (b) Reconnection electric field strength.

projections of the blue and green field lines on to a plane at approximately constant altitude. Reconnection changes the field structure, transforming the blue and green field lines to the pair of red field lines shown.

### 3. Discussion

Based on the modeling results presented we suggest that magnetic reconnection events occurring in Jupiter’s near-planet polar magnetosphere could be responsible for some of the downward electron acceleration that produces Jupiter’s swirl auroras, and possibly also other polar auroral features. Our case is presented below.

#### 3.1. Particle Acceleration Resulting From Reconnection

Magnetic reconnection leads to acceleration of both ions and electrons and forms fast outflow “jets” in the plane of the reconnecting magnetic field components (e.g., Hesse & Cassak, 2020). For the scenario shown in Figure 1c, this plane is at approximately constant altitude, and so we do not expect reconnection jets to impact the atmosphere below. However, magnetic reconnection is also capable of accelerating a fraction of the local ions and electrons to very high energies, particularly along the magnetic field. Because Jupiter’s UV polar auroras are thought to be caused by energetic electron precipitation, and since upward field-aligned electron beams have been widely reported at higher altitudes (e.g., Paranicas et al., 2018), the production of magnetic-field-aligned electron beams is of particular interest (e.g., Drake et al., 2006; Egedal et al., 2012). This is illustrated in Figure 1c.

The energy release rate scales with the reconnection electric field strength (the reconnection rate), appearing to correlate with the typical energy of electrons in these magnetic-field-aligned beams. Reconnection electric fields of  $1\text{--}10 \text{ mV m}^{-1}$  in space anti-sunward of the Earth has been observed to produce electron energies up to hundreds of keV (e.g., Oieroset et al., 2002), whereas electric field strengths of order  $1 \text{ V m}^{-1}$  in the solar corona are thought to produce MeV electrons (e.g., Holman, 2005). Figure 4b shows that possible reconnection electric fields in Jupiter’s near-planet polar magnetosphere span these values, approaching solar-corona-like strengths of  $\sim 1 \text{ V m}^{-1}$  on occasion. This suggests typical electron beam energies of a few-hundred keV to a few MeV, and so the potential downward electron beams illustrated in Figure 1c could be capable of generating polar auroras.

The brightness of the resulting UV emissions would depend on the precipitating energy flux, which is difficult to similarly constrain via comparison with reported observations of reconnection in space. However, the proposed physics should also produce electron beams directed upward, potentially explaining some of

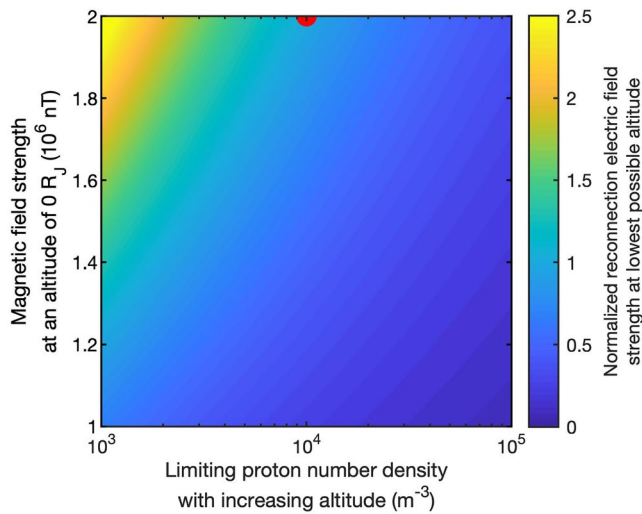


**Figure 5.** Analysis of the sensitivity of reconnection electric field strengths to the magnetic field strength at an altitude of  $0 R_J$  and the limiting proton number density with increasing altitude. The red semi-circle indicates the nominal model parameters. The color scale indicates the reconnection electric field strength at the lowest possible reconnection altitude, normalized to the value for the nominal model parameters.

should be positively correlated with the magnetic field strength at lower altitudes (Connerney et al., 2018). The present version of our theory alone does not provide an obvious explanation for the dependence of all electron beam detections on the phase of Jupiter’s rotation (Bonfond et al., 2018). In addition, similarly field-aligned proton beams are also possible as a result of reconnection (e.g., Kronberg et al., 2012). If this possibility is found to be consistent with spacecraft observations at higher altitudes then this would have further, distinct implications for atmospheric chemistry and auroral emissions from Jupiter’s polar regions (see the review by Badman et al. (2015) and references therein).

### 3.2. Robustness of the Present Model

Although we have used a highly simplified description of the polar magnetosphere it nonetheless captures the key features of the environment that lead to our proposed explanation for some of the polar auroras. For example, including a more precise variation in current layer thickness with decreasing altitude would not affect the principle that these layers become thinner as the magnetic field becomes stronger. The most poorly constrained model parameter is the limiting proton number density with increasing altitude, and so sensitivity to this is assessed in Figure 5. The red semi-circle indicates the region of this parameter space that we have considered so far (Connerney et al., 2018; Saur et al., 2018), corresponding to a reference reconnection electric field strength at the lowest possible reconnection altitude for an arbitrary shear between upper-boundary point motions. The color scale shows the equivalent reconnection electric field strength normalized to this reference value, using the same shear. Maintaining the same magnetic field strength at an altitude of  $0 R_J$  and increasing or decreasing the limiting proton number density by an order of magnitude leads to reconnection electric field strengths that are  $\sim 3$  times smaller and  $\sim 3$  times larger, respectively. We suggest this is a modest variation, especially given that a density of  $10^5 \text{ m}^{-3}$  approaches densities typical of Jupiter’s equatorial plasma sheet (e.g., Bagenal, 1992).

### 3.3. Triggering Perturbations From the Distant Magnetosphere

The magnetic flux threading the swirl regions maps to distances of order hundreds of  $R_J$  from the planet and likely deeper into the magnetotail, where there are potential sources of the perturbations that could trigger near-planet polar reconnection. Note that we prefer the term “trigger,” since the energy released in

the upward beams observed by the *Juno* spacecraft at higher altitudes. Energy fluxes associated with these detected upward beams can be as high as order  $100 \text{ mW m}^{-2}$  (Ebert et al., 2019), and so if we assume some of these were produced by the physics that we propose then the expectation of similar downward electron beam energy fluxes provides an indication that precipitating energy fluxes are high enough to produce polar emissions like those observed.

While the ability of magnetic reconnection to accelerate particles is well established, conditions in Jupiter’s near-planet polar magnetosphere are unlike those in other space environments in which the process has been extensively observed (e.g., Hesse & Cassak, 2020). For this reason, our conclusion is tentative. Numerical modelling of magnetic reconnection under such a strong “guide” magnetic field is beyond the scope of the present study but would be highly relevant in future, particularly for interpreting if any of the upward electron beams observed by the *Juno* spacecraft can be attributed to this physics. Note that electron acceleration during reconnection can involve contracting magnetic islands that produce power-law electron distributions (e.g., Drake et al., 2006) and can be due to magnetic-field-aligned electric fields (e.g., Egedal et al., 2012).

If future work can identify a subset of observed beams caused by near-planet polar reconnection then the hypothesis that these beams should correspond to simultaneous polar auroras in magnetically conjugate regions can be tested, as well as the expectation that beam energies

any near-planet polar reconnection is present in the polar magnetic field itself, only requiring an incoming signal to produce conditions that allow a fraction of the energy to be released. It is important to recognize that only “large-scale” Alfvénic disturbances could lead to such reconnection, and not smaller scale wave activity. This is because the time taken for the reconnection-related plasma flow pattern to be established is controlled by an Alfvén speed associated with the reconnecting magnetic field component, typically of order 10–100 km s<sup>-1</sup>, whereas Alfvén waves propagate along the magnetic field lines at approximately the speed of light near the planet (see Figure 2b). Reconnection should therefore only occur at a location if the field deflection persists for long enough, which will only apply to sufficiently long magnetic-field-aligned wavelengths.

The triggering perturbations are therefore likely due to sustained shears between distant plasma flow regimes. For a distant magnetotail source, the necessary flow shears on scales of order 10s to 100s of R<sub>J</sub> appear to be consistent with observations made by the *New Horizons* spacecraft (McComas et al., 2017). Note also that such long distances along magnetic field lines from the relatively low-Alfvén-speed regime of the distant magnetosphere to the relativistic-Alfvén-speed regime near the planet leads to Alfvén wave travel times that are so long that transfer of information is effectively only directed from the former to the latter, on timescales over which the triggering physics may vary. This is particularly significant at Jupiter, which has the largest magnetosphere in the Solar System, and may enhance the ability of distant magnetospheric dynamics to trigger near-planet reconnection.

### 3.4. Why Only Jupiter’s Polar Regions, Why Not Also at Earth and Saturn?

The short answer to this question is because energy release rates are only high enough in the very strong magnetic field regime of Jupiter’s near-planet polar regions. We have highlighted that the reconnection electric field is dependent on the square of the reconnection magnetic field, which is limited by the background magnetic field strength. This is explored in Figure 5 where we use weaker magnetic field strengths at an altitude of 0 R<sub>J</sub> in our model, quantifying the reduction in reconnection electric fields. The range considered in this figure approximates Jupiter’s polar to equatorial field strengths near the planet, showing that there should be a strong preference for sufficiently high energy release rates in the polar regions. Finally, because the equivalent field strengths at the Earth and Saturn are ~50 times weaker this physics at those planets should be associated with upper-limit reconnection rates of order 0.1 mV m<sup>-1</sup>, leading to negligible electron acceleration and potentially explaining why Jupiter has the brightest polar auroras. If this theory is supported by future observational tests then it may be possible to extrapolate to astrophysical systems, with implications for the search for exoplanetary auroras. This potential physics could become non-negligible at planets with polar magnetic field strengths that are ~40 times higher than Earth’s, or greater.

### Data Availability Statement

Derived data shown in Figures 2–5 are publicly available in the *Zenodo* data repository (<https://doi.org/10.5281/zenodo.5082189>).

### References

- Badman, S. V., Branduardi-Raymont, G., Galand, M., Hess, S. L. G., Krupp, N., Lamy, L., et al. (2015). Auroral processes at the giant planets: Energy deposition, emission mechanisms, morphology and spectra. *Space Science Reviews*, 187, 99–179. <https://doi.org/10.1007/s11214-014-0042-x>
- Bagenal, F. (1992). Giant planet magnetospheres. *Annual Review of Earth and Planetary Sciences*, 20, 289–328. <https://doi.org/10.1146/annurev.ea.20.050192.001445>
- Behannon, K. W., Lepping, R. P., & Ness, N. F. (1983). Structure of dynamics of Saturn’s outer magnetosphere and boundary regions. *Journal of Geophysical Research*, 88, 8791–8800. <https://doi.org/10.1029/ja088ia11p08791>
- Bhardwaj, A., & Gladstone, R. G. (2000). Auroral emissions of the giant planets. *Reviews of Geophysics*, 38, 295–353. <https://doi.org/10.1029/1998rg000046>
- Bonfond, B., Gladstone, G. R., Grodent, D., Gérard, J. C., Greathouse, T. K., Hue, V., et al. (2018). Bar code events in the Juno-UVS data: Signature ~10 MeV electron microbursts at Jupiter. *Geophysical Research Letters*, 45, 12108–12115. <https://doi.org/10.1029/2018gl080490>
- Bonfond, B., Gladstone, G. R., Grodent, D., Greathouse, T. K., Versteeg, M. H., Hue, V., et al. (2017). Morphology of the UV aurorae Jupiter during Juno’s first perijove observations. *Geophysical Research Letters*, 44, 4463–4471. <https://doi.org/10.1002/2017gl073114>
- Cassak, P. A., & Shay, M. A. (2007). Scaling of asymmetric magnetic reconnection: General theory and collisional simulations. *Physics of Plasmas*, 14, 102114. <https://doi.org/10.1063/1.2795630/10.102114>

### Acknowledgments

A. Masters and J. Stawarz are supported by Royal Society University Research Fellowships. H. Manners is supported by a Royal Society PhD studentship. W. Dunn is supported by a Science and Technology Facilities Council (STFC) research grant to University College London (UCL) and by European Space Agency (ESA) contract no. 4000120752/17/NL/MH.

- Clark, G., Mauk, B. H., Haggerty, D., Paranicas, C., Kollmann, P., Rymer, A., et al. (2017). Energetic particle signatures of magnetic field-aligned potentials over Jupiter's polar regions. *Geophysical Research Letters*, *44*, 8703–8711. <https://doi.org/10.1002/2017GL074366>
- Connerney, J. E. P., Kotsiaros, S., Oliverson, R. J., Espley, J. R., Joergensen, J. L., Joergensen, P. S., et al. (2018). A new model of Jupiter's magnetic field from Juno's first nine orbits. *Geophysical Research Letters*, *45*, 2590–2596. <https://doi.org/10.1002/2018gl077312>
- Cowley, S. W. H., & Bunce, E. J. (2001). Origin of the main auroral oval in Jupiter's coupled magnetosphere-ionosphere system. *Planetary and Space Science*, *49*(1), 1067–1088. [https://doi.org/10.1016/S0032-0633\(00\)00167-7](https://doi.org/10.1016/S0032-0633(00)00167-7)
- Cowley, S. W. H., Bunce, E. J., Stallard, T. S., & Miller, S. (2003). Jupiter's polar ionospheric flows: Theoretical interpretation. *Geophysical Research Letters*, *30*(5), 1220. <https://doi.org/10.1029/2002gl016030>
- Delamere, P. A., & Bagenal, F. (2010). Solar wind interaction with Jupiter's magnetosphere. *Journal of Geophysical Research*, *115*, A10201. <https://doi.org/10.1029/2010ja015347>
- Drake, J. F., Swisdak, M., Che, H., & Shay, M. A. (2006). Electron acceleration from contracting magnetic islands during reconnection. *Nature*, *443*, 553–556. <https://doi.org/10.1038/nature05116>
- Ebert, R. W., Allegrini, F., Bagenal, F., Bolton, S. J., Connerney, J. E. P., Clark, G., et al. (2017). Spatial distribution and properties of 0.1–100 keV electrons in Jupiter's polar auroral region. *Geophysical Research Letters*, *44*, 9199–9207. <https://doi.org/10.1002/2017gl075106>
- Ebert, R. W., Greathouse, T. K., Clark, G., Allegrini, F., Bagenal, F., Bolton, S. J., et al. (2019). Comparing electron energetics and UV brightness in Jupiter's northern polar region during Juno perijove 5. *Geophysical Research Letters*, *46*, 19–27. <https://doi.org/10.1029/2018gl081129>
- Egedal, J., Daughton, W., & Le, A. (2012). Large-scale electron acceleration by parallel electric fields during magnetic reconnection. *Nature Physics*, *8*, 321–324. <https://doi.org/10.1038/nphys2249>
- Elliott, S. S., Gurnett, D. A., Kurth, W. S., Clark, G., Mauk, B. H., Bolton, S. J., et al. (2018). Pitch angle scattering of upgoing electron beams in Jupiter's polar regions by whistler mode waves. *Geophysical Research Letters*, *45*, 1246–1252. <https://doi.org/10.1002/2017gl076878>
- Elliott, S. S., Gurnett, D. A., Kurth, W. S., Mauk, B. H., Ebert, R. W., Clark, G., et al. (2018). The acceleration of electrons to high energies over the Jovian polar cap via whistler mode wave-particle interactions. *Journal of Geophysical Research: Space Physics*, *123*, 7523–7533. <https://doi.org/10.1029/2018JA025797>
- Elliott, S. S., Gurnett, D. A., Yoon, P. H., Kurth, W. S., Mauk, B. H., Ebert, R. W., et al. (2020). The generation of upward-propagating whistler mode waves by electron beams in the Jovian polar regions. *Journal of Geophysical Research: Space Physics*, *125*, e2020JA027868. <https://doi.org/10.1029/2020JA027868>
- Gérard, J.-C., Bonfond, B., Mauk, B. H., Gladstone, G. R., Yao, Z. H., Greathouse, T. K., et al. (2019). Contemporaneous observations of Jovian energetic auroral electrons and ultraviolet emissions by the Juno spacecraft. *Journal of Geophysical Research*, *124*, 8298–8317. <https://doi.org/10.1029/2019ja026862>
- Grodent, D. (2015). A brief review of ultraviolet auroral emissions on giant planets. *Space Science Reviews*, *187*, 23–50. <https://doi.org/10.1007/s11214-014-0052-8>
- Grodent, D., Bonfond, B., Yao, Z., Gérard, J.-C., Radioti, A., Dumont, M., et al. (2018). Jupiter's aurora observed with HST during Juno orbits 3 to 7. *Journal of Geophysical Research*, *123*, 3299–3319. <https://doi.org/10.1002/2017ja025046>
- Grodent, D., Clarke, J. T., Waite, J. H., Jr., Cowley, S. W. H., Gérard, J.-C., & Kim, J. (2003). Jupiter's polar auroral emissions. *Journal of Geophysical Research*, *108*(A10), 1366. <https://doi.org/10.1029/2003ja010017>
- Haewasantati, K., Bonfond, B., Wannawichian, S., Gladstone, G. R., Hue, V., Versteeg, M. H., et al. (2021). Morphology of Jupiter's polar auroral bright spot emissions via Juno-UVS observations. *Journal of Geophysical Research*, *126*, e2020JA028586. <https://doi.org/10.1029/2020ja028586>
- Hesse, M., & Cassak, P. A. (2020). Magnetic reconnection in the space sciences: Past, present, and future. *Journal of Geophysical Research*, *125*, e2018JA025935. <https://doi.org/10.1029/2018ja025935>
- Hill, T. W. (2001). The Jovian auroral oval. *Journal of Geophysical Research*, *106*, 8101–8107. <https://doi.org/10.1029/2000ja000302>
- Hinson, D. P., Flasar, F. M., Kliore, A. J., Schinder, P. J., Twicken, J. D., & Herrera, R. G. (1997). Jupiter's ionosphere: Results from the first Galileo radio occultation experiment. *Geophysical Research Letters*, *24*, 2107–2110. <https://doi.org/10.1029/97gl01608>
- Holman, G. (2005). Energetic electrons in solar flares as viewed in X-rays. *Advances in Space Research*, *35*, 1669–1674. <https://doi.org/10.1016/j.asr.2004.11.022>
- Hue, V., Greathouse, T. K., Gladstone, G. R., Bonfond, B., Gérard, J. C., Vogt, M. F., et al. (2021). Detection and characterization of circular expanding UV-emissions observed in Jupiter's polar auroral regions. *Journal of Geophysical Research*, *126*, e2020JA028971. <https://doi.org/10.1029/2020ja028971>
- Isbell, J., Dessler, A. J., & Waite, J. H., Jr. (1984). Magnetospheric energization by interaction between planetary spin and the solar wind. *Journal of Geophysical Research*, *89*, 10716–10722. <https://doi.org/10.1029/ja089ia12p10716>
- Kronberg, E. A., Kasahara, S., Krupp, N., & Woch, J. (2012). Field-aligned beams and reconnection in the Jovian magnetotail. *Icarus*, *217*, 55–65. <https://doi.org/10.1016/j.icarus.2011.10.011>
- Mauk, B. H., Clark, G., Gladstone, G. R., Kotsiaros, S., Adriani, A., Allegrini, F., et al. (2020). Energetic particles and acceleration regions over Jupiter's polar cap and main aurora: A broad overview. *Journal of Geophysical Research*, *125*, e2019JA027699. <https://doi.org/10.1029/2019ja027699>
- Mauk, B. H., Haggerty, D. K., Paranicas, C., Clark, G., Kollmann, P., Rymer, A. M., et al. (2017). Discrete and broadband electron acceleration in Jupiter's powerful aurora. *Nature*, *549*, 66–69. <https://doi.org/10.1038/nature23648>
- McComas, D. J., Allegrini, F., Bagenal, F., Ebert, R. W., Elliott, H. A., Nicolaou, G., et al. (2017). Jovian deep magnetotail composition and structure. *Journal of Geophysical Research*, *122*, 1763–1777. <https://doi.org/10.1002/2016ja023039>
- Miller, S., Rego, D., Achilleos, N., Stallard, T. S., Prangé, R., Dougherty, M., et al. (2000). Infrared spectroscopic studies of the Jovian ionosphere and aurorae. *Advances in Space Research*, *26*, 1477–1488. [https://doi.org/10.1016/s0273-1177\(00\)00081-8](https://doi.org/10.1016/s0273-1177(00)00081-8)
- Nichols, J. D., Clarke, J. T., Gérard, J. C., & Grodent, D. (2009). Observations of Jovian polar auroral filaments. *Geophysical Research Letters*, *36*, L08101. <https://doi.org/10.1029/2009gl037578>
- Nichols, J. D., Clarke, J. T., Gérard, J. C., Grodent, D., & Hansen, K. C. (2009). Variation of different components of Jupiter's auroral emission. *Journal of Geophysical Research*, *114*, A06210. <https://doi.org/10.1029/2009ja014051>
- Oieroset, M., Lin, R., Phan, T., Larson, D. E., & Bale, S. D. (2002). Evidence for electron acceleration up to 300 keV in the magnetic reconnection diffusion region of Earth's magnetotail. *Physical Review Letters*, *89*, 195001. <https://doi.org/10.1103/physrevlett.89.195001>
- Paranicas, C., Mauk, B. H., Haggerty, D. K., Clark, G., Kollmann, P., Rymer, A. M., et al. (2018). Intervals of intense energetic electron beams over Jupiter's poles. *Journal of Geophysical Research*, *123*, 1989–1999.
- Prangé, R. (1992). The UV and IR Jovian aurorae. *Advances in Space Research*, *12*, 379–389. [https://doi.org/10.1016/0273-1177\(92\)90413-r](https://doi.org/10.1016/0273-1177(92)90413-r)

- Saur, J., Janser, S., Schreiner, A., Clark, G., Mauk, B. H., Kollmann, P., et al. (2018). Wave-particle interaction of Alfvén waves in Jupiter's magnetosphere: Auroral and magnetospheric particle acceleration. *Journal of Geophysical Research*, *123*, 9560–9573. <https://doi.org/10.1029/2018ja025948>
- Stallard, T. S., Clarke, J. T., Melin, H., Miller, S., Nichols, J. D., O'Donoghue, J., et al. (2016). Stability within Jupiter's polar auroral "Swirl region" over moderate timescales. *Icarus*, *268*, 145–155. <https://doi.org/10.1016/j.icarus.2015.12.044>
- Waite, J. H., Grodent, D., Mauk, B. M., Majeed, T., Gladstone, G. R., Bolton, S. J., et al. (2000). Multispectral observations of Jupiter's aurora. *Advances in Space Research*, *26*, 1453–1475. [https://doi.org/10.1016/s0273-1177\(00\)00089-2](https://doi.org/10.1016/s0273-1177(00)00089-2)
- Zhang, B., Delamere, P. A., Yao, Z., Bonfond, B., Lin, D., Sorathia, K. A., et al. (2021). How Jupiter's unusual magnetospheric topology structures its aurora. *Science Advances*, *7*, eabd1204. <https://doi.org/10.1126/sciadv.abd1204>